Hindawi
Advances in Civil Engineering
Volume 2020, Article ID 9631804, 16 pages
https://doi.org/10.1155/2020/9631804

Research Article

Seismic Damage Rapid Assessment of Road Networks considering Individual Road Damage State and Reliability of Road Networks in Emergency Conditions

Jinlong Liu,[1,2] **Hanxi Jia**,[1] **Junqi Lin**,[1] **and Heng Hu**[1]

[1]*Key Laboratory of Earthquake Engineering and Engineering Vibration, Institute of Engineering Mechanics, China Earthquake Administration, Harbin 150080, China*
[2]*Heilongjiang Provincial Key Laboratory of Underground Engineering Technology, Harbin 150086, China*

Correspondence should be addressed to Jinlong Liu; liuliu_jinlong@163.com

Received 23 February 2020; Revised 28 June 2020; Accepted 21 July 2020; Published 6 August 2020

Academic Editor: Xue Zhang

Road networks are one of the vital components of a transportation system that influence the traffic capacity and disaster losses after the earthquakes. The road network reliability is crucial for the postearthquake emergency decision-making. In this study, a method is proposed to assess the seismic damage of road networks considering individual road damage state and reliability of road networks in emergency conditions. First, we assess the importance of the factors that affect seismic road damage using the AdaBoost algorithm. In addition, artificial neural networks are used to evaluate the damage state of an individual road based on the factors that are selected with higher importance. Then, the improved estimation for the reliability of road networks is adopted to assess the damage of road networks. Last, the method is demonstrated using the road networks in Karamay, China.

1. Introduction

Lifeline systems refer to the infrastructure networks, including transportation, communication, water supply, drainage, power supply, gas supply, and oil transportation, which have a major impact on social life and production [1]. The road networks are one of the critical components of the transportation system that transmit information in the lifeline systems. They are also the life passage for seismic relief after the earthquake. Rapidly and accurately assessing the damage state of the road networks after the earthquake can provide reference information for the deployment of emergency rescue works and rationally distribute the manpower and material resources for disaster relief. A timely rescue can reduce the casualties and property losses in the disaster areas.

In recent years, the seismic damage evaluations of the transportation networks have been widely investigated by some studies. In these past studies, most of them regard bridge failure as the main factor affecting the capacity of the road network, while ignoring the impact of road failure on the overall performance of the road network [2]. Kiremidjian et al. proposed an assessment model of the transportation networks based on the loss evaluation of the bridges [3]. Guo et al. considered the roads as the main components of the transportation systems in their method, which were developed according to postdisaster traffic demand [4]. However, the focus of the research proposed by Guo et al. remained the bridges. Some researchers have focused studies on the road networks. The method proposed by Cheng et al. was based on the road network capacity (RNC) model and combined travel demand model, which was mainly calculated by the original-destination (OD) matrix [5]. It is only required to solve the shortest path traffic reliability between all OD sets and OD sets of the road networks [6]. The expected value of the traffic probability of all the shortest paths [7] is the connectivity reliability of the road network, which can be used to evaluate the overall operation of the road networks after the earthquake. The method can reflect the structure and evaluate the traffic capacity of the road network. However, as road network vertices increase, the calculation of the number of OD sets will increase exponentially [8], which will greatly increase the workload of assessment. Hence, a faster calculation method is needed to assess the road capacity after the earthquake.

Furthermore, the damage assessments of the individual road were ignored in most previous studies [9–11]. Pitilakis et al. investigated the dynamic transportation performance directly based on the whole road networks [10]. Some studies are used to evaluate the road seismic damage based on the linear regression model [12]. The causes of the road damages are very complicated, and they are not only influenced by the earthquakes. However, the linear models are still flawed in solving the problem of very complicated internal mechanism, and they often need some assumptions. In recent years, the rises of machine learning algorithms have greatly advanced the development of the prediction problems [13]. For example, the ANN model was used to assess the bridge damage severity quantification [14] and buildings' damage seismic state [15]. The ANN model also has almost no application in the road network seismic damage assessment. Before using the ANN model to predict, the features should be screened first rather than by empirically selecting the influencing factors [12]. One of the best ways to choose the factors that influence road damage is to assess the importance of them [16]. The method of ensemble learning algorithms has been proved to have a good performance in the analysis of feature importance [16–18]. There are many algorithms in the ensemble learning models, such as the most commonly used random forest algorithm [19] and adaptive boosting algorithm (AdaBoost) [20]. However, ensemble learning models have not been used to assess the importance of different influencing factors of seismic road damage.

This paper shows a method for the seismic damage assessment of road networks considering the damage state of an individual road and reliability of road networks. The first part of this method consists of two models: (1) the assessment of factor importance applying the AdaBoost algorithms [20] and (2) the estimation of the damage state of an individual road using the ANN model based on the results of the AdaBoost model. The second part is to evaluate the reliability of road networks considering the capacity of road networks (RNC) and pass probability based on the results of the ANN model. Finally, we use a case study to verify the applicability of the method proposed in this study, and it is proved that the method has a good performance on the problem of the seismic damage assessment of road networks.

2. Data

Because the data of the road are less than the bridge in an earthquake, some studies have to make some assumptions so as to verify the efficiency of their method. The data used in this article are derived from actual seismic damage and do not contain any assumptions. The road damage data were collected by the government and some institutions (Sichuan Highway Planning, Survey and Design Institute, China Highway Planning and Design Institute, and Shanxi Highway Planning Survey and Design Institute). They were all derived from the 2008 Ms 8.0 Wenchuan earthquake in China (Table 1). In Table 1, the seismic fortification intensity and soil type refer to the "Chinese Specification of Seismic Design for Highway Engineering" (JTG B02-2013) [21], and the practical intensity refers to the Chinese seismic intensity scale (GBT 17742-2008) [22].

There were five national highways (G108, G212, G213, G317, and G318) and eleven provincial highways (S101, S105, S106, S202, S205, S210, S211, S301, S302, S303, and S306) in the disaster-stricken areas of Sichuan province damaged to varying degrees. National road G213, provincial road S302, and provincial road S303 crossing the area of earthquake intensity VIII were seriously damaged, and the total damage of rural roads was about 24,103 kilometers. There were two national highways (G212 and G316) and nine provincial highways (S205, S206, S208, S219, S306, S307, S313, X482, and X484) in Gansu province which were damaged to varying degrees, and the total damage was about 5518 kilometers including rural roads. There were only one national highway (G108) and two provincial highways (S210 and S309) in Shanxi province which were damaged to varying degrees, and the total damage was about 1,791 kilometers including rural roads. The above roads were divided into 63 links based on the damage and mileage. Figure 1 demonstrates some typical damages of the road in the Wenchuan earthquake, which were divided into some road segments and had the individual number [24].

3. Assessment of Seismic Road Damage

3.1. Select Factors. There are many factors affecting road seismic damage, but not every factor is critical. In the rapid assessment of road damage, the most important factors should be selected for evaluation, which can save time in obtaining data and running procedures.

The road is mainly composed of subgrade and pavement, retaining structure, and slope. The road damage is divided into three types based on the failure parts: subgrade damage, supporting structure damage, and slope damage. The seismic damage data show that the three seismic types are not independent. For example, the retaining structure or subgrade will be destroyed when the slope collapses. The following is a detailed description of the selection factors (Figure 2) (Tables 2 and 3):

(1) Different road grades have different importance in seismic design. According to the Chinese Design Code of Highway Subgrades (JTG D30-2015) [25], the road can be divided into 4 grades. For each grade, the road has different materials and construction methods, and so, the earthquake resistance ability of each grade road is different.

(2) Subgrade-related factors included the subgrade type and height difference of the subgrade [26]. The type of subgrade was classified according to the form of excavation and filling. The subgrade height difference is the difference between the design elevation of the subgrade centerline and the original ground

Table 1: The damage roads of the Wenchuan earthquake with some characteristics; the number consists of the road name and the mileage number.

Number	Height difference (m)	Road grades	Supporting and retaining type	Seismic fortification intensity	Practical intensity (degree)	Slope height (m)	Soil type of the site
G213: K1020 + 960	10.4	3	Gravity-type grouted	VII	XI	13.6	II
G213: K1018 + 600	1.2	3	Gravity-type grouted	VII	XI	40.0	I
G213: K1022 + 900	15.6	3	Reinforced retaining wall	VII	XI	0	I
G213: K1029 + 850	3.1	3	Gravity-type grouted	VII	X	33.0	I
G213: K1008 + 900	3.0	3	Gravity-type grouted	VII	XI	20.0	I
G213: K1014 + 175	6.0	3	Gravity-type grouted	VII	XI	0	I
G213: K1008 + 400	2.0	3	Cutting slope	VII	XI	50.0	III
G213: K1008 + 580	9.9	3	Gravity-type concrete	VII	XI	50.0	III
G213: K1012 + 400	13.6	3	Gravity-type concrete	VII	XI	15.5	III
G213: K1029 + 700	6.2	3	Gravity-type concrete	VII	X	50.0	III
G213: K1023 + 700	2.2	3	Prestressed cable	VII	XI	19.0	III
G213: K1009 + 080	7.1	3	Cutting slope	VII	XI	0	III
G213: K1008 + 980	4.0	3	Gravity-type concrete	VII	XI	0	III
G213: K916 + 508	3.6	3	Cutting slope	VII	IX	7.0	III
G213: K37 + 350	1.8	2	Gravity-type grouted	VII	X	294.0	II
G213: K38 + 500	1.0	2	Gravity-type grouted	VII	X	326.3	II
G213: K40 + 100	3.6	2	Gravity-type grouted	VII	X	121.2	I
G213: K42 + 400	4.4	2	Facing wall	VII	X	175.5	II
G213: K26 + 800	1.5	2	Cutting slope	VII	XI	24.3	I
G213: K73 + 000	2.0	2	Cutting slope	VII	IX	175.9	I
G213: K29 + 950	1.0	2	Facing wall	VII	XI	19.7	I
G213: K34 + 140	1.5	2	Cutting slope	VII	XI	122.7	III
G213: K35 + 600	3.9	2	Cutting slope	VII	XI	100.0	III
G213: K50 + 200	3.0	2	Cutting slope	VII	X	480.1	III
G213: K58 + 160	3.4	2	Gravity-type grouted	VII	X	15.0	III
G213	1.5	3	Gravity-type grouted	VII	IX	7.1	III
G213	1.7	3	Gravity-type grouted	VII	IX	92.1	II
G213	4.0	3	Gravity-type grouted	VII	IX	27.0	II
G213	3.4	3	Cutting slope	VII	IX	93.4	III
G213	2.3	3	Facing wall	VII	IX	71.0	III
G213	1.5	3	Gravity-type grouted	VII	IX	0	II
G213	1	3	Gravity-type grouted	VII	IX	10.0	II
G213	1.2	3	Cutting slope	VII	IX	0	II

Table 1: Continued.

Number	Height difference (m)	Road grades	Supporting and retaining type	Seismic fortification intensity	Practical intensity (degree)	Slope height (m)	Soil type of the site
S303: K10 + 341	1.8	2	Gravity-type grouted	VII	X	5.0	III
S303: K28 + 941	0.5	2	Gravity-type grouted	VII	X	50.0	II
S303: K40 + 500	0.5	2	Gravity-type grouted	VII	IX	27.4	III
S303: K16 + 441	2.6	2	Cutting slope	VII	X	237.5	II
S303: K31 + 841	1.0	2	Cutting slope	VII	IX	28.7	I
S303: K36 + 600	1.0	2	Cutting slope	VII	IX	100.0	III
S303: K43 + 200	1.0	2	Cutting slope	VII	IX	30.0	II
S303: K26 + 900	3.1	2	Gravity-type grouted	VII	IX	25.0	III
S302	2.0	2	Cutting slope	VII	IX	27.0	III
S302: K732 + 560	1.5	2	Gravity-type grouted	VII	X	7.4	III
S302	2.5	2	Facing wall	VII	X	47.5	I
S105	2.2	3	Gravity-type grouted	VII	XI	2.8	I
S105	3.1	3	Gravity-type grouted	VII	XI	25.3	III
S105	3.5	3	Facing wall	VII	XI	36.7	I
S105: K167 + 460	5.9	3	Cutting slope	VII	XI	8.4	III
S105: K168 + 900	7.4	3	Cutting slope	VII	XI	9.0	III
XU09	2.3	4	Gravity-type concrete	VI	X	44.3	II
S210	1.3	3	Gravity-type grouted	VII	VII	324.4	I
S210	3.7	3	Cutting slope	VII	VII	63.6	II
S210	2.3	3	Cutting slope	VII	VII	24.4	III
G212	4.2	3	Gravity-type grouted	VII	VIII	34.3	II
G213	1.0	2	Gravity-type grouted	VII	VIII	20.3	I
S303	3.8	4	Cutting slope	VII	VII	194.3	III
S303	4.2	4	Gravity-type grouted	VII	VIII	35.0	III
G317	1.5	3	Cutting slope	VII	VII	173.3	II
G317	2.5	2	Gravity-type grouted	VII	VI	2.5	II
G317	2.4	2	Gravity-type grouted	VII	VI	5.0	I
G317	0.5	2	No	VII	VI	0	III
G317	6.0	2	Gravity-type grouted	VII	VI	0	III

elevation, which was used to describe the stability of the subgrade in the earthquake. The diagrammatic drawing of the subgrade type is shown in Figure 2.

(3) The retaining structures are used to support and stabilize the subgrade filling or slope to prevent soil slipping and thus to maintain soil stability [27]. The retaining structure can be divided into gravity retaining wall and flexible retaining wall. Gravity retaining wall can be divided into three types according to the construction method: dry masonry, wet masonry, and concrete. The seismic damage data show that the dry masonry retaining wall is more prone to serious damage, and its actual seismic capacity is obviously weaker than that of wet and concrete, so the dry masonry retaining wall and the nonretaining wall are combined into one category. The reinforced retaining wall, antislide pile, and anchor cable structure with good seismic performance are classified as advantageous retaining, so the retaining types are divided into four categories: nonretaining, wet masonry gravity, concrete gravity, and advantageous retaining.

(4) The site soil has a great influence on the bearing capacity of the foundation [28]. In the Wenchuan earthquake, a large number of shoulder walls were inclined and deformed due to insufficient bearing capacity of the foundation. According to the Specification of Seismic Design for Highway Engineering (JTG B02-2013) [21], the engineering site is divided into four categories, as shown in Table 2.

(5) Slope-related factors select slope angle, height, and protective measures. As the slope height and slope increase, the number of earthquake damage

Figure 1: The typical damage of the road in the Wenchuan earthquake, including the retaining wall being cut, the wall body being inclined outward, the subgrade being buried by the rock, and the subgrade partially collapsed [23].

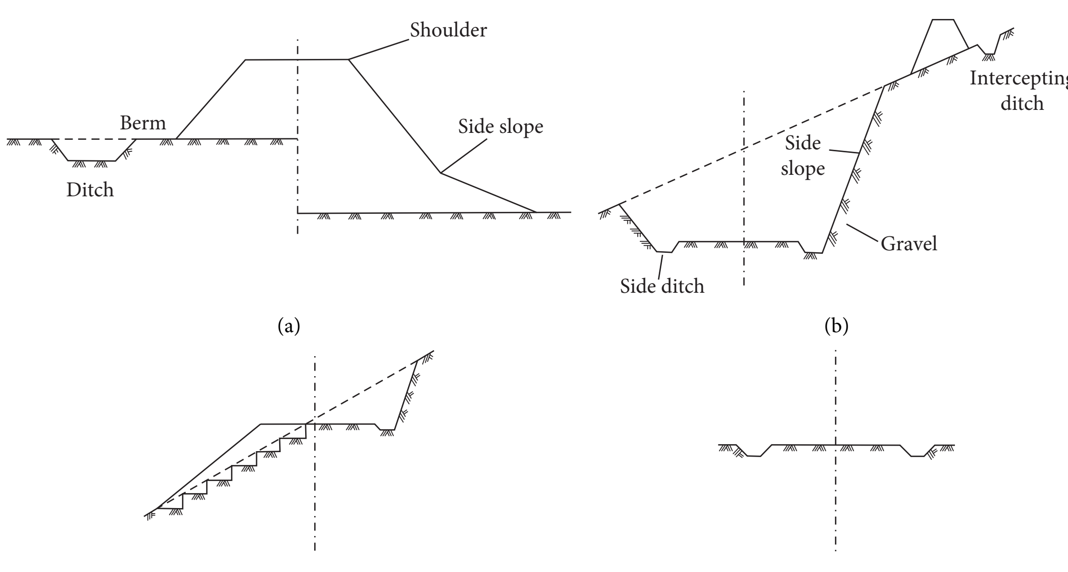

Figure 2: Diagrammatic drawing of the subgrade type. (a) Embankment. (b) Cutting. (c) Half-filled and half-dug. (d) No digging and no filling.

Table 2: Classification of engineering sites.

Mean shear wave velocity (m/s)	Site category			
	I	II	III	IV
$v_{se} > 500$	0	—	—	—
$500 \geq v_{se} > 250$	< 5	≥ 5	—	—
$250 \geq v_{se} > 140$	< 3	≥ 3, ≤ 50	> 50	—
$v_{se} \leq 140$	< 3	≥ 3, ≤ 15	> 15, ≤ 80	> 80

Table 3: Classification of slope protection types.

Classification	Slope protection type
Level I	No protection, wall protection, plant protection, spraying (no net)
Level II	Net hanging, shotcrete, active and passive protection net
Level III	Frame beam, prestressed anchor (cable) protection, composite measures

increases simultaneously. The higher the slope is, the more obvious the acceleration amplification effect is under the action of the earthquake, which is easy to produce earthquake damage such as rock projectile. Similarly, the steeper the slope is, the worse the stability will be. In the Wenchuan earthquake, the slope damage mainly concentrates on the slope between 35° and 65°. In addition, the characteristics of seismic damage show that the seismic damage of the slope mainly occurs on the soil slope without protection, while the failure of the slope with the combination of the frame, anchor bolt, and multi-measures is less. This indicates that appropriate protective measures can effectively reduce the degree and quantity of damage to the slope. According to the slope protection method, slope protection can be divided into three categories, as shown in Table 3; from type I to type III, the seismic protection capability of the slope is gradually enhanced.

(6) The seismic intensity describes the intensity of the earthquake. The damage data of the Wenchuan earthquake also show that the amount and extent of damage increase with the increase of intensity, which is consistent with our understanding. The seismic fortification level is an important factor of road's seismic resistance ability. In the engineering design stage, the seismic resistance of the road will be guaranteed according to the corresponding specifications [21]. Therefore, the fortification intensity can be taken as one of the evaluation indexes.

Above all, we estimated the importance of ten factors as follows: highway classification, subgrade type, supporting and retaining type, soil type of the site, slope height, slope angle, protective measure, height difference of subgrade, seismic fortification intensity, and practical intensity (Table 4).

3.2. Assessment of the Factor Importance Applying the AdaBoost Algorithm. There are many algorithms for assessing the importance of features in the machine learning domain, such as support vector machine, AdaBoost algorithm, and decision tree model. This study selected the AdaBoost algorithm in ensemble learning. The essence of the ensemble learning model is to combine many weak processors to get a better predictive processor. Ensemble learning model works well for large data set and insufficient data set. The data in this study are not sufficient. Common ensemble learning models are of two types: bagging algorithms and boosting algorithms. The boosting algorithm predicts through a series of aggregated estimated model weighted averages. AdaBoost is a representative algorithm in the boosting algorithm [29]. In this study, the input parameters were ten factors and five damage states. The damage states of individual roads are divided into five levels: none, slight, moderate, extensive, and complete [30].

The procedures of the AdaBoost algorithm can be summarized as follows:

(i) Step 1: initialize the sample weights and perform equal weight processing.
(ii) Step 2: train the base classifier. The weights are updated according to the results of each decision tree and then trained until the conditions are met.
(iii) Step 3: the weighted average method is used to combine the base classifiers into strong classifiers, and the decision trees with smaller errors are more weighted.

Base classifier: classification and regression tree classifier (maximum depth = 10, minimum sample leaf = 5, algorithm = SAMME.R, number of estimators = 200, and learning rate = 0.5).

Due to the small data set, we chose the cross validation function in the sklearn function library to validate the model rather than dividing the data set into training set and testing set. The mean average accuracy of the output classification was 0.8204, which was higher than the accuracy of the AdaBoost algorithm in other models [16]. Figure 3 presents the importance of the ten factors, and there are five factors that have the importance value more than 10%.

3.3. Artificial Neural Network Assessment Model. In the rapid assessment after the earthquake, the assessment speed is one of the most important points. Reducing the parameters can

Table 4: Factors of seismic road damage.

Factors	Classification	Features
Highway classification	Expressway	Better seismic performance
	First-class	Better seismic performance
	Second-class	
	Third-class	Failure occurs more frequently
	Fourth-class	Failure occurs more frequently
Subgrade type	No digging and no filling	No damage
	Cutting	Destruction accounts for 26% of the total damage
	Embankment	Destruction accounts for 28% of the total damage
	Half-filled and half-dug	Failure occurs most frequently (48%)
Supporting and retaining type	Reinforced retaining wall, prestressed cable, facing wall	Beneficial to mitigating damage
	Gravity-type concrete	Failure occurs most frequently
	Gravity-type wet masonry	More serious damage
	No	Not conducive to mitigating damage
Soil type of the site	I	
	II	
	III	Intensifying the damage slightly
	IV	Intensifying the damage
Slope height (h)	0 m	The least number of damages occurred
	$0\,\mathrm{m} < h \le 15$	Less destruction occurs
	$15\,\mathrm{m} < h \le 40\,\mathrm{m}$	
	$40\,\mathrm{m} < h \le 120\,\mathrm{m}$	More susceptible to damage
	$120\,\mathrm{m} < h$	More susceptible to damage
Slope angle (θ)	0°	The least number of damages occurred
	$0^\circ < \theta \le 35^\circ$	
	$35^\circ < \theta \le 65^\circ$	Failure occurs most frequently
	$65^\circ < \theta$	More susceptible to damage
Protective measure	No, steening retaining wall	Not conducive to resisting seismic, small quantity
	Frame beam, precast block	Beneficial to seismic
	Hanging net and guniting, safety netting system	Can resist part of seismic
	Shotcrete, mortar	Not conducive to resisting seismic
Height difference of subgrade	$h \le 1\,\mathrm{m}$	
	$1\,\mathrm{m} < h \le 3\,\mathrm{m}$	
	$3\,\mathrm{m} < h \le 5\,\mathrm{m}$	
	$5\,\mathrm{m} < h$	
Seismic fortification intensity	VI	
	VII	
	VIII	
	IX	
Practical intensity	VI	
	VII	
	VIII	
	IX	
	X	
	XI	

reduce the amount of data and speed up the evaluation. Therefore, we used the AdaBoost algorithm to evaluate the importance of different influencing factors. According to the results of Section 3.2, we selected the five most important factors as input parameters. We chose practical intensity, supporting and retaining type, height difference of subgrade, slope height, and soil type of the site as the input parameters. The sum of the importance value of these five parameters reached 80%. Hence, we ignore other parameters when establishing the evaluation model. ANN has strong adaptive, self-learning, and nonlinear mapping capabilities, which can solve the problem of less data and uncertainty, and is not limited by nonlinear models. Earthquake is an accidental event, and destructive earthquakes have a lower probability of occurrence, such as the Wenchuan earthquake. Therefore, there are small data set on road damages and great uncertainties. Moreover, the relationship between various influencing factors of road damage and the results of damage is not clear. Above all, artificial neural networks are suitable for road damage assessment. A typical neural network includes an input layer, an implicit layer, and an output layer. The layers are fully connected, and there is no connection between the layers. The hidden layer can have one or more layers. For a typical network, a single layer of hidden layers is sufficient [13]. The input and output layers have been determined. The hidden layer selects a layer based on the actual amount of data. The number of hidden layer neurons is determined according to the following empirical equation:

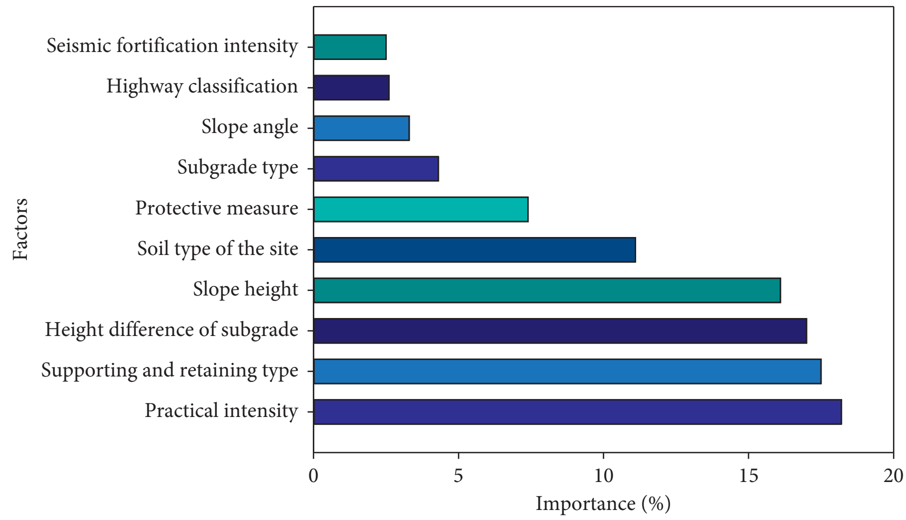

Figure 3: The importance values of factors of the seismic road damage based on the AdaBoost algorithm.

$$L = \sqrt{n + m} + a, \tag{1}$$

where L is the number of hidden layers, n and m are the number of input and output layers, respectively, and a is a constant between 1 and 10. $n = 10$ and $m = 1$. We determined the number of hidden layer neurons as ten according to the convergence speed and accuracy during the training process. Therefore, this study selected the most typical three-layer backpropagation neural network, with 5 input layer neurons, 10 hidden layer neurons, and 1 output layer neuron (Figure 4). The maximum epochs were 10,000, and the learning rate was 0.1 based on the running processing and the data set. The mean square error loss function and sigmoid function were selected as the cost function (2) and activation function (3) of the hidden layer, respectively:

$$y = \frac{1}{n} \sum (\hat{y} - t)^2, \tag{2}$$

where y is the value of the cost function, n presents the amount of the roads, $\hat{y}$ is the damage state of the ANN model, and t is the actual damage state.

$$f_{(x)} = \frac{1}{1 + e^{-z}}, \tag{3}$$

where $f_{(x)}$ is the ReLU function, and x is the input of the ReLU function.

We selected 50 roads as the training set and the remaining 12 roads as the testing set. The model was run in the Jupyter Notebook of the Anaconda Navigator environment with python 3 languages (https://www.anaconda.com/). The accuracy of the linear model was 87% [8], while the accuracy of the ANN model was 92%. It can be seen that the ANN model had a good performance in assessing road damage problems.

4. Analysis on the Reliability of Road Networks

According to the results of the ANN model, we could obtain the damage state of each individual road. However, it is also necessary to consider the damage of the road network so that the road could not affect the emergency rescue after the earthquake. The combination of the damage state on the individual road and reliability of road networks can ensure that the lifeline system of emergency rescue after the earthquake is unimpeded. Therefore, we proposed the postearthquake evaluation method of the reliability of road networks.

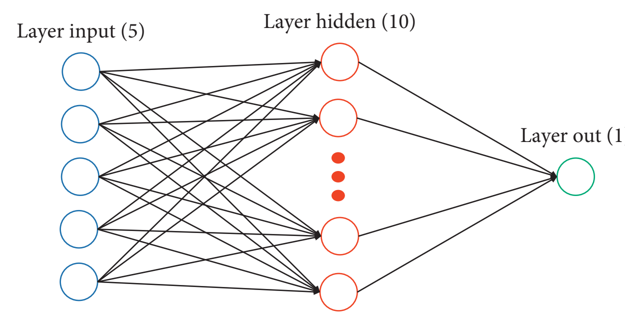

Figure 4: Layout for artificial neural networks for the assessment model.

4.1. The Pass Possibility of an Individual Road. A strong earthquake caused damage to the roads. Earthquake damage index is usually used to describe the damage degree of road, but the damage degree of earthquake is only the description of the physical damage state of road, and it cannot reflect the status of road traffic function. Therefore, it is necessary to establish the relationship between seismic damage index and pass probability. The results of Section 3.3 gave only the damage state and could not directly obtain the pass probability, $P_{r,i}$, of an individual road. Therefore, we used the damage index [31] as the conversion indicator to translate the damage state into pass possibility. Table 5 shows the relationship between the damage index and the damage state. The damage index and pass probability had a certain range, and we decided to use the median value of them as the value of the damage index and $P_{r,i}$.

4.2. Reliability of the Road Network Model. According to the results of the ANN model, we could obtain the damage state of each individual road. However, it is also necessary to consider the damage of the road network so that the road could not affect the emergency rescue after the earthquake. Therefore, we proposed the postearthquake evaluation method of the reliability of road networks. Urban RNC is an important decision indicator in urban road network planning and construction [4]. The RNC represents the maximum traffic volume and provides important information for effective traffic flow control and demand management. The RNC is the maximum flow rate determined according to the geometric characteristics of the road, traffic conditions, and specified operational characteristics, and its value has relative stability and prescriptiveness. The simplest consideration for RNC is to add up the maximum capacity of all road links to get the physical capacity of an urban transportation network. Under the general road and traffic conditions of the city and when not affected by the intersection of planes, the possible RNC, N_P, can be computed by [32]

$$N_P = \frac{3600}{\delta_i}, \tag{4}$$

where δ_i is the average traffic interval between consecutive traffic. When the city does not have the value of δ_i, the road capacity can use the value in Table 6.

According to the code for design of urban road engineering, in road capacity design, the actual capacity of the road is not allowed to reach the maximum capacity value. Instead, it tends to reduce the maximum capacity as the design value for safety. The higher the level of the road, the greater the reduction coefficient. When the RNC is not affected by a plane intersection, the design RNC, N_{i0}, can be computed by

$$N_{i0} = a_c \times N_P, \tag{5}$$

where a_c is the road classification coefficient of the vehicle lane (Table 7).

The initial RNC, N_0, before the earthquake is defined as follows:

$$N_0 = \sum_{i=1}^{n} Z_i \times N_{i0}, \tag{6}$$

where Z_i is the importance index of the i-th road, which mainly reflects the importance or influence of the road in the network. The urban road network consists of several road sections, but each road section has different importance in the whole road network. Some road sections have high utilization rate, and some are very low. The impact of these unit sections on the connectivity of the entire road network is not the same. Therefore, the weight of the unit road link needs to be calibrated. The index Z_i is usually calculated based on the betweenness centrality. However, the betweenness centrality involves calculation in a complex network [33]. Hence, the index Z_i can be expressed as (7) for the convenience of calculation and speed of the assessment:

$$Z_i = \frac{B_i}{B_{t\quad d}}, \tag{7}$$

where B_i is the number of road links connected to the i-th road link and $B_{t\quad d}$ is the total number of road links. If the road link contains bridges, tunnels, etc., the pass probability $P_{r,i}$ is obtained based on the ANN model, and the RNC after the earthquake can be obtained by (8). The reliability of the road network, R, is defined as the ratio of N to N_0 (9). Table 8 presents the reliability state of the road network, including reliable, medium reliable, and unreliable.

$$N = \sum_{i=1}^{n} P_{r,i} \times Z_i \times N_{i0}, \tag{8}$$

$$R = \frac{N}{N_0}. \tag{9}$$

Table 5: The relationship between the damage index and the damage state.

Damage state	Damage index (I)	Pass state	Pass probability (p)
None	$0.00 \le I < 0.10$	Allowable	$0.90 < p \le 1.00$
Slight	$0.10 \le I < 0.30$	Limitation	$0.70 < p \le 0.90$
Moderate	$0.30 \le I < 0.55$	Limitation	$0.45 < p \le 0.70$
Extensive	$0.55 \le I < 0.85$	Unallowed	$p \le 0.001$
Complete	$0.85 \le I \le 1.00$	Unallowed	$p \le 0.001$

Table 6: Possible capacity of the road [32].

Calculated driving speed (km/h)	50	40	30	20
N_P (pcu/h)	1690	1640	1550	1380

5. Case Study Results

The methodology proposed in this paper is applied to the Karamay district in Karamay city, China. Due to the lack of information on the roads of all cities and for the propose of demonstrating the method proposed in this study, the reliability of road networks is applied to the area enclosed by the Zhunger road, Xihuan road, Nanhuan road, and Donghuan road, as shown in Figure 5. The road network contains 64 road links and 39 nodes, totaling 60 km (Table 9).

According to the artificial neural network assessment model obtained in Section 3, the failure states of all units in the road network under different earthquake intensities can be obtained, and the seismic damage index for each road is shown in Table 10.

The reliability of each road link under different seismic intensities is obtained based on Section 4.1. Figure 6 presents the road network reliability with the intensity of VI, VII, VIII, and IX, respectively. From the figure, it can be observed that the reliability of the road network in intensity VI is very

Table 7: Coefficient of the road classification [24].

Road classification	Expressway	Arterial road	Minor arterial road	Branch road
a_c	0.75	0.80	0.85	0.90

Table 8: The reliability state of the road network.

Reliability state	Reliable	Medium reliable	Unreliable
Reliability of the road network	$R \geq 0.8$	$0.5 \leq R < 0.8$	$R < 0.5$

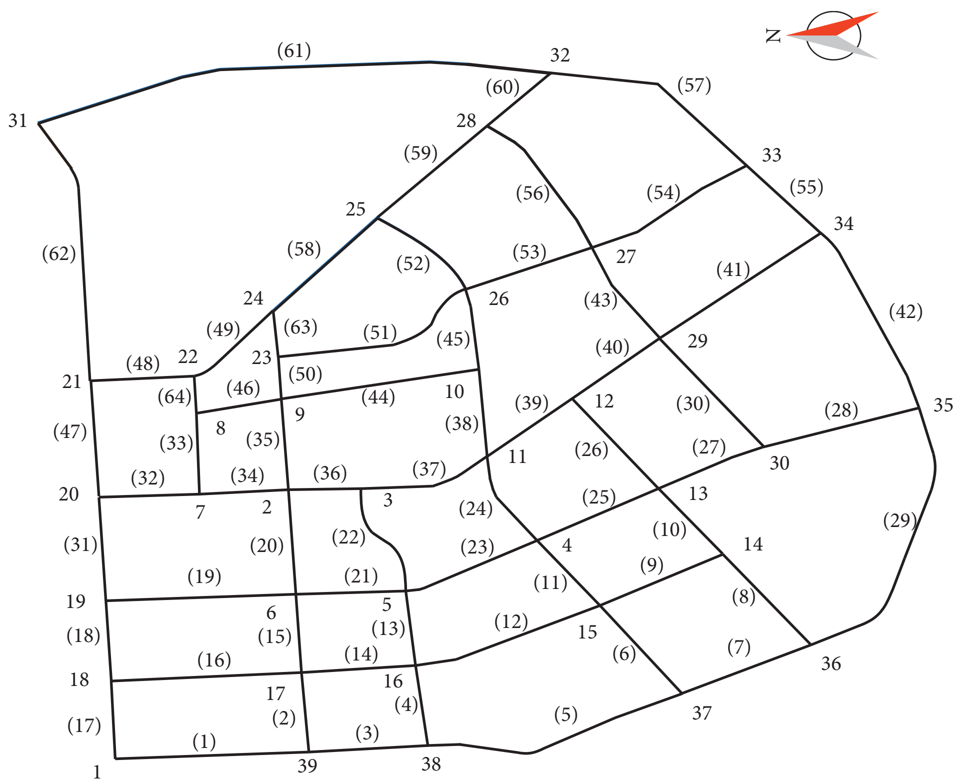

Figure 5: Road network plan.

Table 9: Properties of the road network.

Road links	Vertex i	Vertex j	Name	Road classification	Length (m)	Year built
1	1	39	Xihuan road	Arterial road	1112	2000
2	17	39	Kunlun road	Arterial road	682	2003
3	38	39	Xihuan road	Arterial road	697	2000
4	16	38	Xingfu road	Arterial road	701	2002
5	37	38	Xihuan road	Arterial road	1625	2000
6	15	37	Nanxin road	Arterial road	903	2002
7	36	37	Xihuan road	Arterial road	864	2000
8	14	36	Shiji road	Arterial road	942	2003
9	14	15	Youjian road	Minor arterial road	846	2003
10	13	14	Shiji road	Arterial road	685	2003
11	4	15	Nanxin road	Arterial road	675	2002
12	15	16	Youjian road	Minor arterial road	1190	2003
13	5	16	Xingfu road	Arterial road	651	2002
14	16	17	Youjian road	Minor arterial road	670	2003
15	6	17	Kunlun road	Arterial road	681	2003
16	17	18	Youjian road	Minor arterial road	1108	2003

Table 9: Continued.

Road links	Vertex i	Vertex j	Name	Road classification	Length (m)	Year built
17	1	18	Zhunger road	Arterial road	680	2003
18	18	19	Zhunger road	Arterial road	700	2003
19	6	19	Youyi road	Arterial road	1106	2003
20	2	6	Kunlun road	Arterial road	914	2003
21	5	6	Youyi road	Arterial road	640	2003
22	3	5	Xingfu road	Arterial road	964	2002
23	4	5	Yingbin road	Arterial road	884	2000
24	4	11	Nanxin road	Arterial road	802	2002
25	4	13	Yingbin road	Arterial road	833	2000
26	12	13	Shiji road	Arterial road	929	2003
27	13	30	Yingbin road	Arterial road	717	2000
28	30	35	Yingbin road	Arterial road	955	2000
29	35	36	Xihuan road	Arterial road	2322	2000
30	29	30	Baoshi road	Minor arterial road	1124	2012
31	19	20	Zhunger road	Arterial road	916	2003
32	7	20	Shengli road	Arterial road	592	2003
33	7	8	Ashan road	Minor arterial road	702	2004
34	2	7	Shengli road	Arterial road	512	2003
35	2	9	Kunlun road	Arterial road	802	2003
36	2	3	Shengli road	Arterial road	515	2003
37	2	11	Shengli road	Arterial road	843	2003
38	10	11	Nanxin road	Arterial road	766	2002
39	11	12	Shengli road	Arterial road	696	2003
40	12	29	Shengli road	Arterial road	736	2003
41	29	34	Shengli road	Arterial road	1309	2003
42	34	35	Nanhuan road	Arterial road	1633	2012
43	27	29	Baoshi road	Minor arterial road	889	2012
44	9	10	Dongjiao road	Minor arterial road	1171	2004
45	10	26	Nanxin road	Arterial road	707	2002
46	8	9	Dongjiao road	Minor arterial road	512	2004
47	20	21	Zhunger road	Arterial road	1013	2003
48	21	22	Changzheng road	Arterial road	599	2004
49	22	24	Jinyuan road	Arterial road	754	2000
50	9	23	Kunlun road	Arterial road	370	2003
51	23	26	Baihua road	Minor arterial road	1338	2004
52	25	26	Nanxin road	Arterial road	822	2002
53	26	27	Baihua road	Minor arterial road	820	2004
54	27	33	Ruyi road	Minor arterial road	1160	2004
55	33	34	Nanhuan road	Arterial road	724	2012
56	27	28	Baoshi road	Minor arterial road	1244	2012
57	32	33	Nanhuan road	Arterial road	1503	2012
58	24	25	Jinyuan road	Arterial road	1009	2000
59	25	28	Jinyuan road	Arterial road	1009	2000
60	28	32	Jinyuan road	Arterial road	608	2000
61	31	32	Donghuan road	Arterial road	3091	2000
62	21	31	Zhunger road	Arterial road	2303	2003
63	23	24	Kunlun road	Arterial road	411	2003
64	8	22	Ashan road	Minor arterial road	316	2004

large. With the increase of the seismic intensity, the probabilities of the road network at medium reliable and unreliable become more obvious.

(1) When the seismic intensity is VI, only one road link is in medium reliable. The RNC is almost unaffected, and the traffic order is normal, which can ensure that people can quickly resume normal work and life.

(2) When the seismic intensity is VII, there are 14% of the road links which are in medium reliable, and the rest are in the reliable state. There are no unreliable road links, and the RNC is affected to some extent. The whole transportation function is intact, and relief supplies and ambulance personnel can enter the disaster area at the first time. The normal traffic can be restored after a short period of time.

(3) When the seismic intensity is VIII, there are 59%, 30%, and 11% of the road links which are in the reliable, medium reliable, and unreliable state, respectively. Some road links have lost the RNC, but they can still meet emergency rescue needs.

(4) When the seismic intensity is IX, there are 44%, 33%, and 23% of the road links which are in the reliable,

Table 10: Damage state of elements in the network.

Road links	Vertex *i*	Vertex *j*	Name	VI	VII	VIII	IX
1	1	39	Xihuan road	0.05	0.11	0.32	0.63
2	17	39	Kunlun road	0.01	0.03	0.04	0.09
3	38	39	Xihuan road	0.02	0.04	0.08	0.15
4	16	38	Xingfu road	0.01	0.05	0.12	0.30
5	37	38	Xihuan road	0.04	0.09	0.23	0.43
6	15	37	Nanxin road	0.11	0.34	0.56	0.87
7	36	37	Xihuan road	0.04	0.07	0.21	0.36
8	14	36	Shiji road	0.03	0.06	0.09	0.18
9	14	15	Youjian road	0.04	0.07	0.22	0.37
10	13	14	Shiji road	0.03	0.06	0.09	0.18
11	4	15	Nanxin road	0.14	0.36	0.63	0.95
12	15	16	Youjian road	0.04	0.07	0.24	0.42
13	5	16	Xingfu road	0.11	0.33	0.61	0.91
14	16	17	Youjian road	0.01	0.04	0.09	0.27
15	6	17	Kunlun road	0.04	0.07	0.20	0.43
16	17	18	Youjian road	0.04	0.08	0.27	0.46
17	1	18	Zhunger road	0.06	0.13	0.32	0.57
18	18	19	Zhunger road	0.12	0.38	0.59	0.93
19	6	19	Youyi road	0.13	0.39	0.62	0.95
20	2	6	Kunlun road	0.06	0.15	0.33	0.61
21	5	6	Youyi road	0.06	0.14	0.32	0.60
22	3	5	Xingfu road	0.02	0.08	0.13	0.29
23	4	5	Yingbin road	0.01	0.03	0.08	0.18
24	4	11	Nanxin road	0.01	0.02	0.06	0.13
25	4	13	Yingbin road	0.01	0.02	0.06	0.13
26	12	13	Shiji road	0.01	0.02	0.07	0.15
27	13	30	Yingbin road	0.01	0.02	0.06	0.14
28	30	35	Yingbin road	0.02	0.04	0.08	0.18
29	35	36	Xihuan road	0.02	0.04	0.08	0.18
30	29	30	Baoshi road	0.02	0.05	0.13	0.30
31	19	20	Zhunger road	0.12	0.38	0.59	0.93
32	7	20	Shengli road	0.04	0.08	0.22	0.41
33	7	8	Ashan road	0.04	0.08	0.22	0.41
34	2	7	Shengli road	0.01	0.02	0.04	0.10
35	2	9	Kunlun road	0.06	0.15	0.33	0.61
36	2	3	Shengli road	0.04	0.07	0.22	0.37
37	2	11	Shengli road	0.01	0.03	0.06	0.15
38	10	11	Nanxin road	0.06	0.15	0.33	0.61
39	11	12	Shengli road	0.01	0.02	0.05	0.14
40	12	29	Shengli road	0.01	0.02	0.05	0.14
41	29	34	Shengli road	0.01	0.02	0.05	0.14
42	34	35	Nanhuan road	0.02	0.04	0.08	0.18
43	27	29	Baoshi road	0.08	0.25	0.48	0.77
44	9	10	Dongjiao road	0.01	0.04	0.09	0.27
45	10	26	Nanxin road	0.01	0.02	0.04	0.10
46	8	9	Dongjiao road	0.01	0.04	0.09	0.27
47	20	21	Zhunger road	0.19	0.40	0.71	0.98
48	21	22	Changzheng road	0.01	0.02	0.06	0.12
49	22	24	Jinyuan road	0.01	0.02	0.06	0.12
50	9	23	Kunlun road	0.01	0.02	0.06	0.12
51	23	26	Baihua road	0.01	0.04	0.09	0.27
52	25	26	Nanxin road	0.01	0.02	0.04	0.10
53	26	27	Baihua road	0.01	0.04	0.09	0.27
54	27	33	Ruyi road	0.01	0.04	0.09	0.27
55	33	34	Nanhuan road	0.02	0.04	0.08	0.18
56	27	28	Baoshi road	0.08	0.25	0.48	0.77
57	32	33	Nanhuan road	0.02	0.04	0.08	0.18
58	24	25	Jinyuan road	0.01	0.02	0.06	0.12

Table 10: Continued.

Road links	Vertex *i*	Vertex *j*	Name	VI	VII	VIII	IX
59	25	28	Jinyuan road	0.01	0.02	0.06	0.12
60	28	32	Jinyuan road	0.01	0.02	0.06	0.12
61	31	32	Donghuan road	0.01	0.02	0.05	0.14
62	21	31	Zhunger road	0.01	0.02	0.05	0.14
63	23	24	Kunlun road	0.01	0.02	0.06	0.12
64	8	22	Ashan road	0.01	0.02	0.06	0.12

medium reliable, and unreliable state, respectively. Some road links are blocked and difficult to pass, which is mainly due to the safety distance between the buildings on both sides, and the road is not enough. The debris piling after the collapse of the buildings has a great impact on the RNC. Fortunately, most of the buildings and the roads have sufficient safety distance, and the road conditions are good due to the reasonable planning of the Karamay district. Hence, there are about half of the road links which are in the reliable state under intensity IX.

We calculated the number of roads connected to each road and the importance index and obtained the RNC before and after the earthquake. Then, the road network reliability under different seismic intensities can be obtained as shown in Table 11.

6. Discussion and Future Works

The rescue time after the earthquakes is crucial. The shorter the time to predict the roads, the faster the rescuer can reach the disaster area, which can greatly reduce casualties and economic losses. Therefore, it is necessary to select suitable factors to assess the roads, which can save the time of collecting data and obtaining suitable accuracy. In this study, we first select ten factors that affect road damage and analyzed their importance using the AdaBoost algorithm. Among ten factors of the road damage, the practical intensity, supporting and retaining type, height difference of subgrade, slope height, and soil type of the site are more important than the others. We chose the five factors as the input variables of the ANN assessment model. The accuracy is more than the regression model [8]. However, the model only considers the data of the Wenchuan earthquake and ignores some factors, such as soil liquefaction, secondary disasters, and economic conditions. Whether the foundation soil in the earthquake is liquefied, it is related to the gravel content, the buried depth of gravel soil, the depth of groundwater, and the seismic intensity [34]. The liquefaction phenomenon does not occur until the earthquake occurs, which is a complex phenomenon, and there is no suitable method to evaluate in a few minutes [3]. Most of the current methods are field surveys. Similarly, secondary disasters also have such problems, and it is unreasonable to use only numerical simulations to predict them [18]. In areas with more developed economies, the more developed the

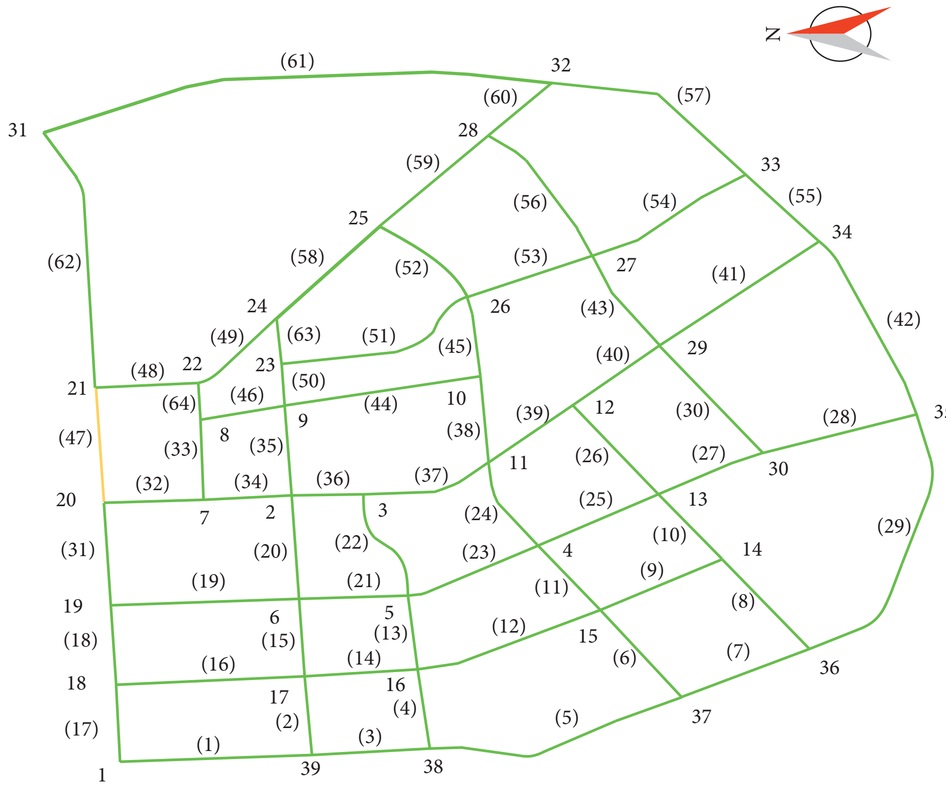

(a)

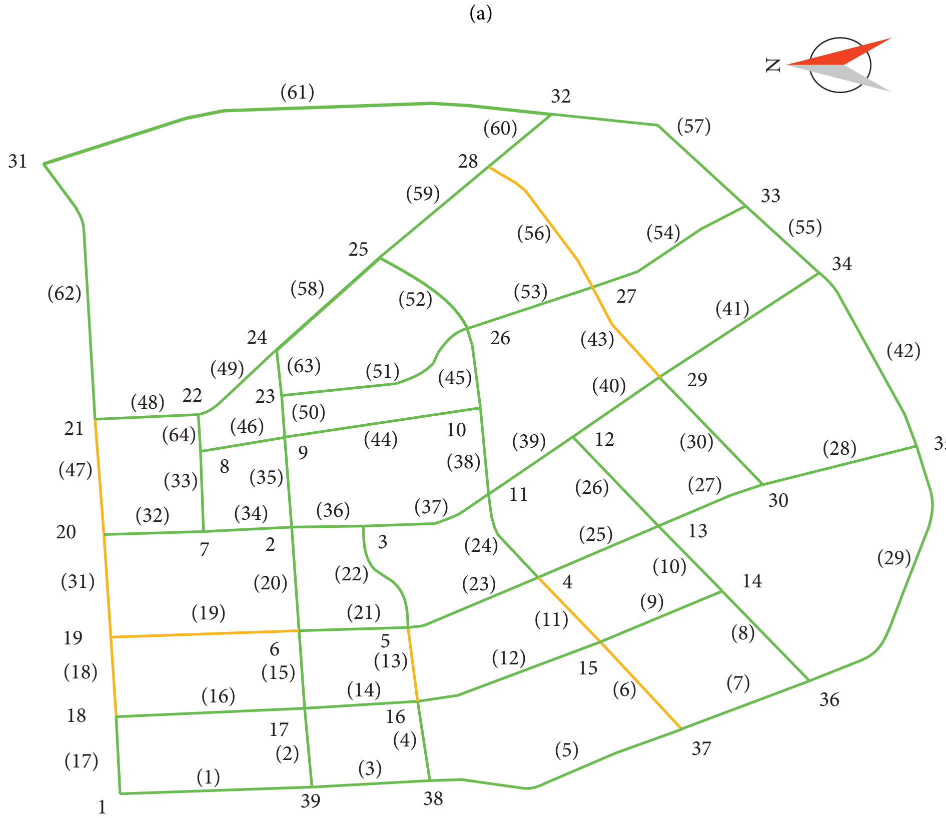

(b)

Figure 6: Continued.

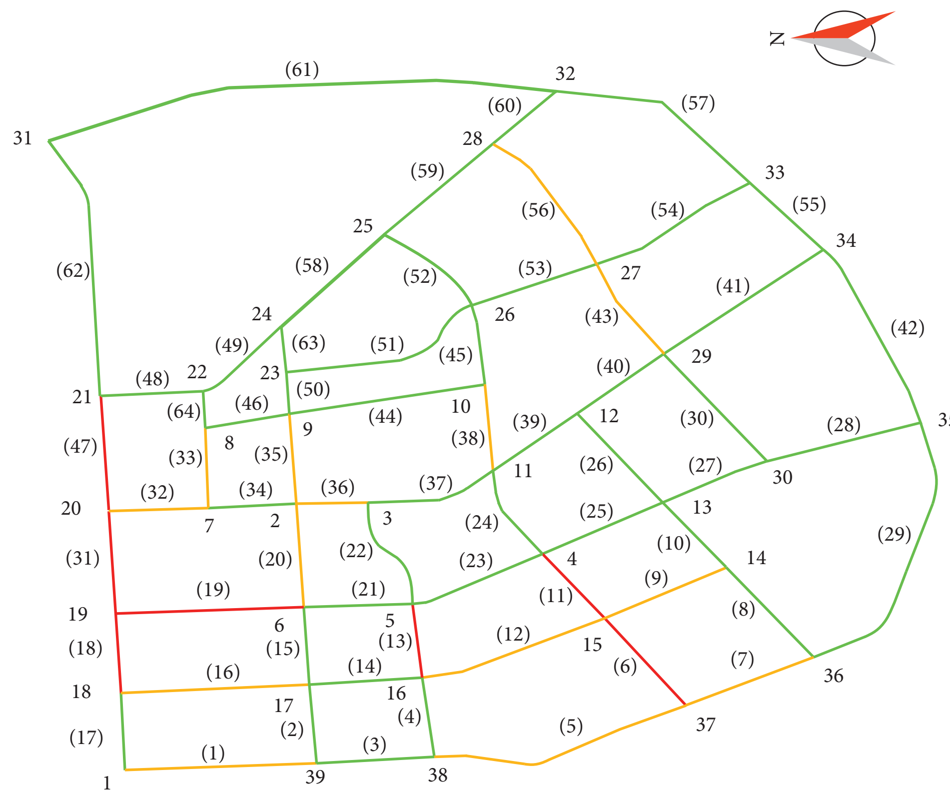

(c)

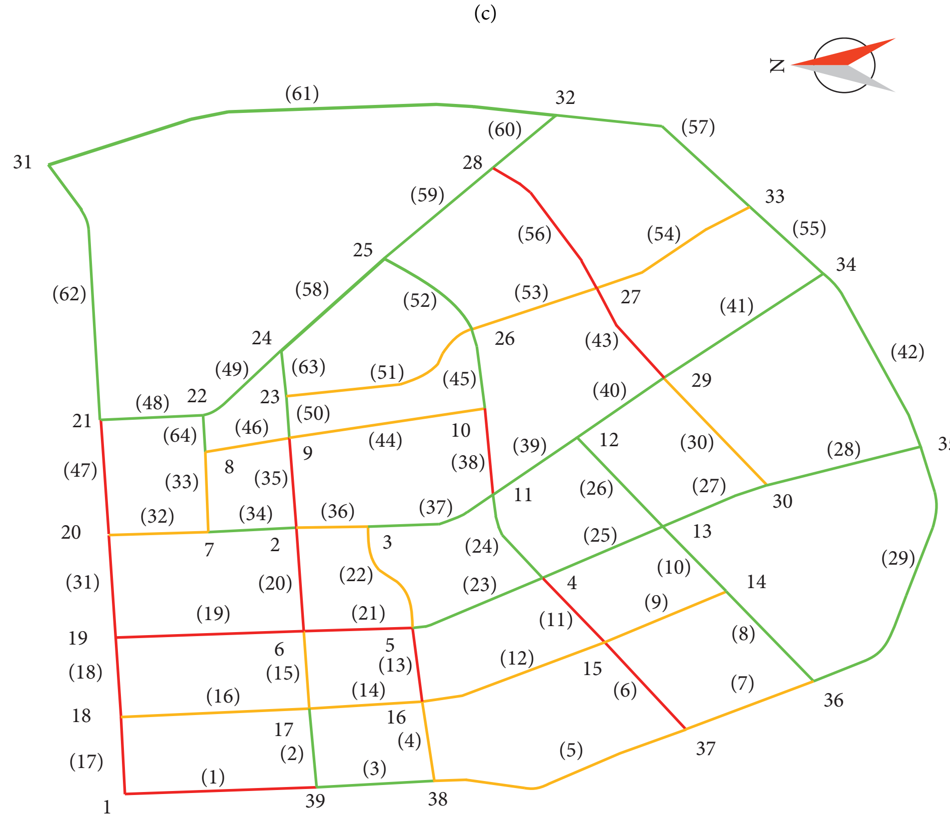

(d)

Figure 6: Road network reliability diagram under different seismic intensities: (a) VI; (b) VII; (c) VIII; (d) IX. Green lines represent the road links being in the reliable state, yellow represents medium reliable, and red represents unreliable.

Table 11: The reliability value corresponding to the seismic intensity of the road network in the Karamay district.

Seismic intensity	VI	VII	VIII	IX
R	0.9299	0.8941	0.7543	0.6631
Reliable state	Reliable	Reliable	Medium reliable	Medium reliable

construction technology, the higher the level of safety of the corresponding roads. The problems in the evaluation of economic conditions are the lack of information, and some data come from many years ago. Annual inflation affects economic conditions [35], so previous data may not apply to the present. Moreover, the small data sets influence the accuracy and applicability of the ANN model. The damage data of the road networks should be further collected in the future earthquakes.

The methodology proposed is more convenient for calculating the reliability of the networks, the speed is faster, and the parameters considered are less than the previous studies [2, 3, 5]. In the evaluation of the road network, we use the median value of the range given by the standard [27] for both the seismic damage index and the pass probability. This part should be optimized in future research to make the predictions more accurate. According to the data, the actual number of earthquake damages is positively correlated with the increase of seismic intensity. The intensity is determined by the macroscopic phenomenon of earthquake damage and the statistical results. The assessment is subjective and ambiguous, and the model using seismic parameters as seismic inputs should be developed, such as the occurrence time, magnitude, and earthquake peak acceleration [10]. Moreover, the method proposed in this study can only evaluate static damage states and road reliability. The dynamic reliability of the road networks ought to be further investigated to reflect the real-time traffic behavior after earthquakes.

7. Conclusions

This paper presents a method to assess the reliability of the road networks considering the factors' importance, damage index, pass possibility, and traffic capacity after the earthquakes. This method is developed based on the machine learning algorithms and linear model. The conclusions of the methodology are as follows: (1) the changes in the practical intensity, supporting and retaining type, height difference of subgrade, slope height, and soil type of the site have a greater impact on the damage of the road. These factors should be considered for the assessment model of the road damage; (2) the seismic intensity has a strong correlation with the damage of the road networks. The greater the seismic intensity, the lower the reliability of the road network and the more serious the damage to the road; and (3) the proposed methodology has a good performance on the evaluation of the road networks. It can be seen that the assessment on the network damages should first consider the individual structure and then calculate the networks.

Data Availability

The data used to support the findings of this study are available from the corresponding author upon request.

Conflicts of Interest

The authors declare that they have no conflicts of interest.

Authors' Contributions

The work in this manuscript was done with the participation of all the authors. Dr. Jinlong Liu was the main planner of the manuscript. The artificial neural network assessment model for an individual road and the analysis model for the reliability of road networks were mainly built by Dr. Liu. However, Ph.D. student Hanxi Jia has also done important work. She was mainly responsible for collecting data of road damage in the Wenchuan earthquake and accomplishing the assessment of the factor importance using the AdaBoost Algorithm. Professor Lin gave them a lot of advice on road damage assessment, and he reviewed the case study results in detail. Postgraduate Heng Hu provided them with detailed data of the road network in Section 5 and helped them to complete the road network reliability analysis.

Acknowledgments

The authors are very grateful to Professor Junqi Lin for his help. This work was supported by the National Key Technology R&D Program of China (grant no. 2018YFC1504401) and the Heilongjiang Provincial Key Laboratory of Underground Engineering Technology Open Project of China (grant no. 2017-HXYKF-06).

References

[1] C. A. Davis, A. Mostafavi, and H. Wang, "Establishing characteristics to operationalize resilience for lifeline systems," *Natural Hazards Review*, vol. 19, no. 4, Article ID 04018014, 2018.

[2] P. Bocchini and D. M. Frangopol, "A stochastic computational framework for the joint transportation network fragility analysis and traffic flow distribution under extreme events," *Probabilistic Engineering Mechanics*, vol. 26, no. 2, pp. 182–193, 2011.

[3] A. Kiremidjian, J. Moore, Y. Y. Fan, O. Yazlali, N. Basoz, and M. Williams, "Seismic risk assessment of transportation network systems," *Journal of Earthquake Engineering*, vol. 11, no. 3, pp. 371–382, 2007.

[4] A. Guo, Z. Liu, S. Li, and H. Li, "Seismic performance assessment of highway bridge networks considering post-disaster traffic demand of a transportation system in emergency conditions," *Structure and Infrastructure Engineering*, vol. 13, no. 12, pp. 1523–1537, 2017.

[5] L. Cheng, M. Du, X. Jiang, and H. Rakha, "Modeling and estimating the capacity of urban transportation network with rapid transit," *Transport*, vol. 29, no. 2, pp. 165–174, 2014.

[6] Y. Ji, R. G. Mishalani, and M. R. McCord, "Estimating transit route OD flow matrices from APC data on multiple bus trips using the IPF method with an iteratively improved base:

method and empirical evaluation," *Journal of Transportation Engineering*, vol. 140, no. 5, Article ID 04014008, 2014.

[7] X. Zhou, M. Venigalla, and S. Zhu, "Bounding box approach to network pruning for efficient path search through large networks," *Journal of Computing in Civil Engineering*, vol. 31, no. 5, Article ID 04017033, 2017.

[8] H. Heng, "Research on assessment method of road seismic damage based on the Wenchuan earthquake," Institute of Engineering Mechanics, China Earthquake Administration, Beijing, China, 2018.

[9] Q. Yu and R. Tian, "Research on reversal lane application method of urban road network based on the Bi-level programming," *Advances in Intelligent Systems and Computing*, Springer, vol. 279, pp. 983–992, Berlin, Germany, 2014.

[10] K. Pitilakis, S. Argyroudis, K. Kakderi, and J. Selva, "Systemic vulnerability and risk assessment of transportation systems under natural hazards towards more resilient and robust infrastructures," *Transportation Research Procedia* in *Proceedings of the 6th Transportation Research Arena*, vol. 14, pp. 1335–1344, Warsaw, Poland, April 2016.

[11] P. Gauthier, A. Furno, and N.-E. El Faouzi, "Road network resilience: how to identify critical links subject to day-to-day disruptions," *Transportation Research Record: Journal of the Transportation Research Board*, vol. 2672, no. 1, pp. 54–65, 2018.

[12] H. Hu, J. Lin, and J. Liu, "Improved methodology for seismic estimation of highway based on Wenchuan earthquake," in *Proceedings of the 2018 International Conference on Modeling, Simulation and Optimization*, pp. 291–296, Xiamen, China, November 2018.

[13] Y. Lecun, Y. Bengio, and G. Hinton, "Deep learning," *Nature*, vol. 521, no. 7553, pp. 436–444, 2015.

[14] P.-j. Chun, H. Yamashita, and S. Furukawa, "Bridge damage severity quantification using multipoint acceleration measurement and artificial neural networks," *Shock and Vibration*, vol. 2015, Article ID 789384, 11 pages, 2015.

[15] K. Morfidis and K. Kostinakis, "Approaches to the rapid seismic damage prediction of r/c buildings using artificial neural networks," *Engineering Structures*, vol. 165, pp. 120–141, 2018.

[16] N. Wang, W. Cheng, M. Zhao, Q. Liu, and J. Wang, "Identification of the debris flow process types within catchments of Beijing mountainous area," *Water*, vol. 11, no. 4, p. 638, 2019.

[17] S. Park and J. Kim, "Landslide susceptibility mapping based on random forest and boosted regression tree models, and a comparison of their performance," *Applied Sciences*, vol. 9, no. 5, p. 942, 2019.

[18] H. Jia, J. Lin, and J. Liu, "An earthquake fatalities assessment method based on feature importance with deep learning and random forest models," *Sustainability*, vol. 11, no. 10, p. 2727, 2019.

[19] B. H. Menze, B. M. Kelm, R. Masuch et al., "A comparison of random forest and its Gini importance with standard chemometric methods for the feature selection and classification of spectral data," *BMC Bioinformatics*, vol. 10, pp. 1–16, 2009.

[20] D. P. Solomatine and D. L. Shrestha, "Adaboost.RT: a boosting algorithm for regression problems," in *Proceedings 2004 IEEE International Joint Conference*, Budapest, Hungary, July 2004.

[21] Code of China, "Chinese specification of seismic design for highway engineering (JTG B02-2013)," Code of China, Beijing, China, 2013.

[22] Code of China, "Chinese seismic intensity scale (GBT 17742-2008)," Code of China, Beijing, China, 2008.

[23] L. Chen, *Report on the Highways' Damage in the Wenchuan Earthquake*, China Communications Press, Beijing, China, 2012.

[24] Code of China, "Code for design of urban road engineering (CJJ 37-2012)," Code of China, Beijing, China, 2012.

[25] Code of China, "Chinese code for design of highway subgrades (JTG D30-2015)," Code of China, Beijing, China, 2015.

[26] D.-s. Ling, Y. Zhao, B. Huang, F. Zhang, and Y. Zhou, "Analysis of dynamic stress path in inhomogenous subgrade under moving aircraft load," *Soil Dynamics and Earthquake Engineering*, vol. 111, no. March 2017, pp. 65–76, 2018.

[27] I. Chowdhury, R. Tarafdar, A. Ghosh, and S. P. Dasgupta, "Seismic response of rectangular liquid retaining structures resting on ground considering coupled soil-structure interaction," *Bulletin of Earthquake Engineering*, vol. 15, no. 9, pp. 3695–3726, 2017.

[28] A. Imtiaz, V. Perron, F. Hollender et al., "Wavefield characteristics and spatial incoherency: a comparative study from argostoli rock-and soil- site dense seismic arrays," *Bulletin of the Seismological Society of America*, vol. 108, no. 5A, pp. 2839–2853, 2018.

[29] D. L. Shrestha and D. P. Solomatine, "Experiments with AdaBoost.RT, an improved boosting scheme for regression," *Neural Computation*, vol. 18, no. 7, pp. 1678–1710, 2006.

[30] China Earthquake Administration, "Classification of earthquake damage to lifeline engineering GB/T 24336-2009," China Standard Press, Beijing, China, 2009.

[31] Standardization Administration and State Administration for Market Regulation, "The Chinese seismic intensity scale GB/T 17742-2008," China Standard Press, Beijing, China, 2008.

[32] Ministry of Housing and Urban-Rural Development of the People's Repulic of China, "Code for design of urban road engineering CJJ 37-2012," China Architecture and Building Press, Beijing, China, 2016.

[33] Z. Safra and U. Segal, "Risk aversion in the small and in the large: calibration results for betweenness functionals," *Journal of Risk and Uncertainty*, vol. 38, no. 1, pp. 27–37, 2009.

[34] M. S. Asadi, R. P. Orense, M. B. Asadi, and M. J. Pender, "Post-liquefaction behavior of natural pumiceous sands," *Soil Dynamics and Earthquake Engineering*, vol. 118, pp. 65–74, 2019.

[35] S. Hatfield-Dodds, H. Schandl, P. D. Adams et al., "Australia is "free to choose" economic growth and falling environmental pressures," *Nature*, vol. 527, no. 7576, pp. 49–53, 2015.